ESD-TR-67-357
Vol. II

MTR-118
Vol. II

COLD LAKE RADIO PROPAGATION AND METEOROLOGICAL EXPERIMENT

(in Three Volumes)

Volume II

Determination of Radio Propagation Conditions from Interferometer and Lake Surface Measurements

AUGUST 1967

L. G. Rowlandson

Prepared for
DEPUTY FOR SURVEILLANCE AND CONTROL SYSTEMS
AEROSPACE INSTRUMENTATION PROGRAM OFFICE
ELECTRONIC SYSTEMS DIVISION
AIR FORCE SYSTEMS COMMAND
UNITED STATES AIR FORCE
L. G. Hanscom Field, Bedford, Massachusetts

Project 7010
Prepared by
THE MITRE CORPORATION
Bedford, Massachusetts
Contract AF19(628)-5165

ESD-TR-67-357
Vol. II

MTR-118
Vol. II

COLD LAKE RADIO PROPAGATION AND METEOROLOGICAL EXPERIMENT

(in Three Volumes)

Volume II

Determination of Radio Propagation Conditions from Interferometer and Lake Surface Measurements

AUGUST 1967

L. G. Rowlandson

Prepared for
DEPUTY FOR SURVEILLANCE AND CONTROL SYSTEMS
AEROSPACE INSTRUMENTATION PROGRAM OFFICE
ELECTRONIC SYSTEMS DIVISION
AIR FORCE SYSTEMS COMMAND
UNITED STATES AIR FORCE
L. G. Hanscom Field, Bedford, Massachusetts

Project 7010

Prepared by
THE MITRE CORPORATION
Bedford, Massachusetts
Contract AF19(628)-5165

FOREWORD

The work reported in the three volumes of this report was supported by the Electronic Systems Division of the Air Force Systems Command, L. G. Hanscom Field, Bedford, Massachusetts, through the MITRE Corporation's Technical Objectives and Plans 7010 - Environmental Factors - under Contracts AF 19(628)-2390 and AF 19(628)-5165.

REVIEW AND APPROVAL

This technical report has been reviewed and is approved.

James F. Shunk

OTIS R. HILL, Colonel, USAF
Director of Aerospace Instrumentation
Program Office

ABSTRACT

Reflection interferometer measurements can be used to describe the propagation conditions affecting the degree of ray-path bending. In combination with these measurements relatively simple meteorological measurements at the lake surface can indicate the magnitude of the refractivity gradient and its vertical extent.

In combination, the two methods appear to provide a technique to determine the effective propagation conditions by direct radio signal diagnosis and with a minimum degree of meteorological support.

ACKNOWLEDGEMENT

The Cold Lake Radio Propagation and Meteorological Experiment was sponsored by the "Joint USAF/RCAF ECCM Evaluation Group."

The participating members in the experiments were designated "The Multipath Propagation Panel" of the above, larger Joint Group. The authors wish to acknowledge the cooperation and coordination provided through the Joint International Group and presently represented by the Canadian and United States cochairmen:

Wing Commander I. Gillean
Director of Electronic Warfare
Canadian Forces Headquarters
Ottawa, Ontario

Mr. R. Creamer
Electronic System Program Analyst
416M/418L
Electronic Systems Division
Bedford, Massachusetts

Financial support was obtained from:

AFHQ-63/70, T & DI-RCAF
AF19(628)-5165 - USAF

The Cold Lake Radio Propagation and Meteorological Experiment is reported in three volumes:

Vol. I - Description of a Radio-Meteorological Experiment to Measure Ray-Path Bending in the Troposphere with a Vertical Interferometer

Vol. II - Determination of Radio Propagation Conditions from Interferometer and Lake Surface Measurements

Vol. III - Description of the Vertical Reflection Interferometer and the Measurement Accuracy

TABLE OF CONTENTS

LIST OF ILLUSTRATIONS

LIST OF TABLES

SECTION I

INTRODUCTION

The Cold Lake radio propagation experiment was designed to measure the effects of propagation conditions on microwave transmissions received through the troposphere. By employing a reflection interferometer technique, the experiment not only permitted the observation of multipath propagation effects but also the determination of the effective ray-path bending.[1] From the radio meteorologist's point of view, the experiment presented an opportunity to measure and explain the propagation conditions which occurred over various times of the day and from week to week. These conditions were then related to their effects on the radio transmissions. To obtain meaningful measurements of the propagation conditions, a coordinated effort was made to cover three areas of meteorological investigation.

The most extensive series of measurements used a C-131 aircraft fitted with probes to measure and record index of refraction directly, as well as other associated parameters such as pressure, temperature, air speed, etc. Details of the installation and its capabilities are given in Appendix I. During the time radio measurements were being made, the aircraft flew a pattern of horizontal and vertical soundings along the radio path. The recorded data were then used to determine the temporal and spatial variations

taking place during the test and to observe fine structure, such as, elevated layers, which could affect radio propagation.

A second effort concentrated on measurements of the surface conditions at Cold Lake from a boat. This data was extremely important in order to observe the variations of the propagation parameters beyond the lower limit of the aircraft measurements.

The final, and very important measurements of the index profile were made using radiosondes. Although fine structure was generally absent from these soundings, it was found that the radiosonde profiles provided a very satisfactory representation of the average propagation conditions. Generally, three soundings were made during each mission, and in addition records were obtained of the surface conditions at launch. These radiosonde soundings assisted in the aircraft calibration at the higher levels and were also used to observe the influx of modifying air masses.

Radio signals received at low angles are generally affected by the propagation conditions in the first few hundred feet of the troposphere. For this reason, a concentrated effort was made to relate the vertical variations of the index of refraction in this region with the local meteorological changes which took place over the surface of Cold Lake. From this analysis it was intended that a certain set of consistent meteorological measurements might be established which would determine and predict the propagation conditions for over-water tests of this kind. At the same time, the

interferometer measurements would hopefully serve as an independent method to determine the propagation environment and to some measure reveal information about the meteorological parameters. The geography of the test area is shown in Figure 1.

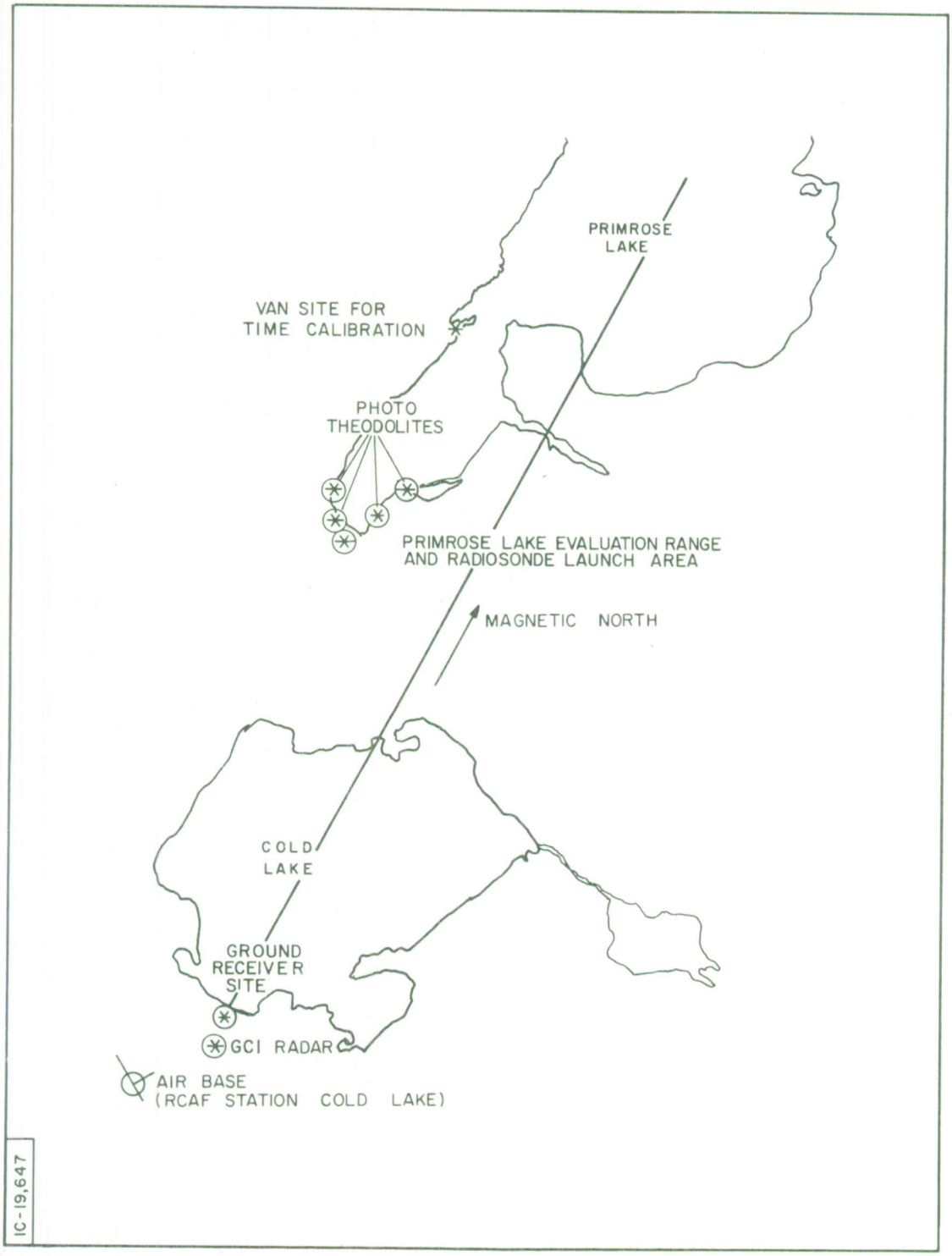

Figure 1. Geography of the Test Area

SECTION II

A REVIEW OF SOME BASIC METEOROLOGICAL PARAMETERS USED TO PREDICT THE VERTICAL INDEX STRUCTURE

The index of radio refraction determines the velocity of electromagnetic propagation and the index gradient normal to the direction of travel determines the amount of bending which occurs.[2] For this experiment, the amount of bending is of most interest because it may define the shape of the vertical index profile.

Within the troposphere, the index of refraction varies only a few hundred parts per million therefore it is convenient to introduce the quantity N ,

$$N = (n - 1) \times 10^6 \tag{1}$$

$$= \frac{77.6}{T} \left[p + \frac{4810e}{T} \right] \qquad \text{[Ref. 3]} \tag{2}$$

where

N = the radio refractivity

n = the radio index of refraction

T = absolute air temperature (deg. Kelvin)

p = air pressure (millibars)

e = partial water vapor pressure (millibars)

It is important to note for later discussion that the saturated water vapor pressure, e_s, is strongly dependent on the air temperature.[4]

During the Cold Lake test period the surface pressure variations were, at most, about 25 parts in a thousand, therefore, the index structure was largely independent of air pressure. Surface air temperature variations were within $10^{\circ}C$ or represented about a 3 percent variation when converted to degrees Kelvin. However, this 3 percent air temperature variation could potentially effect changes in the water vapor pressure as great as $\pm$ 43 percent about an average value. So, it is apparent that the index of refraction variations near the lake surface are greatly dependent on small changes which occur in the local air temperature and on the moisture content and temperature of new, incoming air. For this reason, most of the analysis of surface index variations is concerned with the changes in the water vapor pressure and its dependence on local conditions.

RADIO REFRACTIVITY AT THE WATER SURFACE N_s

The layer of air immediately in contact with the water surface will reach an equilibrium temperature equal to the surface water temperature. It will also adjust its vapor pressure, in accordance with this equilibrium temperature, to approach a completely saturated

condition. Knowing the surface water temperature, therefore, provides an equivalent air temperature under saturated vapor pressure conditions. Using tables relating the saturated vapor pressure with air temperature and knowing the barometric pressure at the surface yields a surface value for refractivity, N_s.[4]

TEMPERATURE EXCESS - T.E.

The relative temperature between the air over the water and the water itself is called the temperature excess.[5]

$$\text{T.E.} = \text{Air Temp.} - \text{Surface Water Temp.} \qquad (3)$$

In the case where warm air passes over cooler water, the temperature excess is positive and the air cooled by surface contact will not rise into the overlying warmer air mass. Conditions are called "stable" and the representative air temperature and humidity above the surface are representative of the air mass before it passed over the water. In the reverse case, where T.E. is negative, instability results. The cool air overriding the water is modified by the vertical motion of the air warmed by the water surface. Increased mixing therefore changes the characteristics of the incoming air and also tends to produce more homogeneous conditions in the vertical. Instability therefore reduces the possibility of having stratified conditions and large vertical index gradients near the surface of the water. There is of course mechanical mixing to consider, which is governed by the wind velocity and fetch or distance of overwater travel. Strong surface winds will increase wave height and surface

roughness. In such a case, even with stable conditions, the mechanical mixing which occurs would make the air more homogeneous near the water surface.

One might therefore conclude that stability and relatively calm wind conditions are a prerequisite for the development of large and horizontally stratified gradients at or near the water surface.

N-DEFICIT

The N-deficit is defined as the difference between the refractivity determined at the water surface N_s and the refractivity of the overlying air mass, N_a, therefore,

$$N.D. = N_s - N_a \qquad (4)$$

If warm, dry air overflows cooler water, the N-deficit will be positive, or superstandard. This is necessarily true because in Equation (2) the water vapor pressure and refractivity of dry air will be less than for saturated air at the water surface. Also, the fact that stability exists will enhance the formation of a superstandard surface layer (surface duct).

If the overlying air is warm and moist, the N-deficit may be either positive (superstandard) or zero (standard). If the N-deficit becomes negative (substandard), there is the possibility of an elevated surface duct forming. Figures 2, 3, and 4 (taken from Ref. 5) show the three possible N-deficit cases under stable conditions.

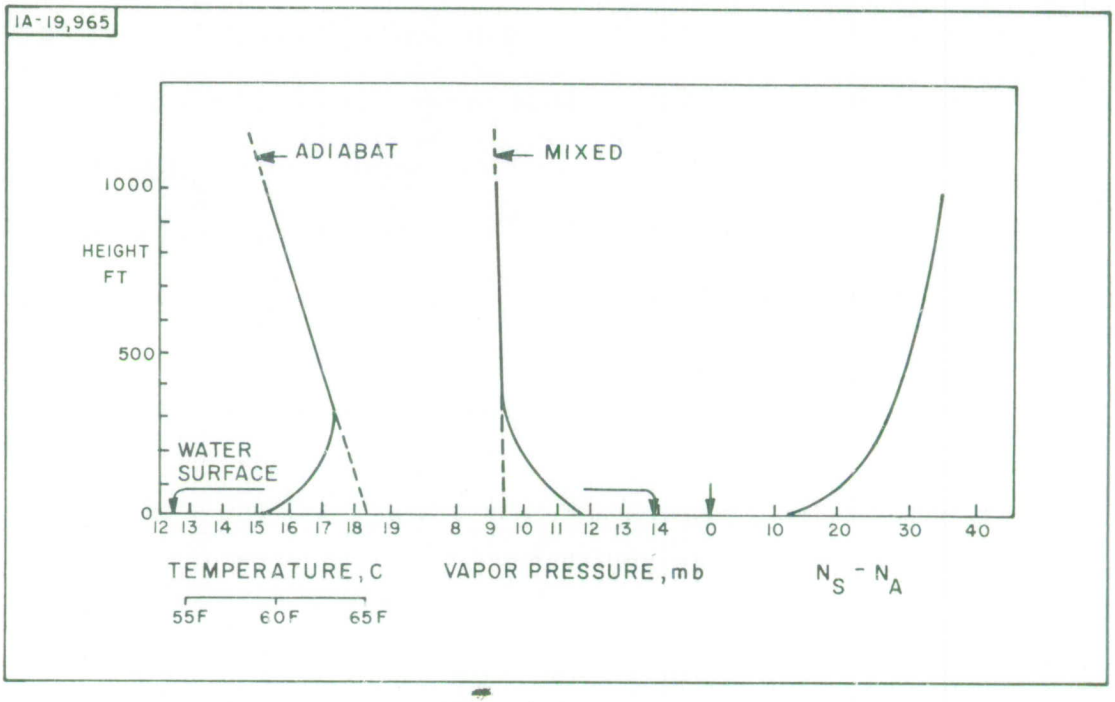

Figure 2. Example of Positive N Deficit

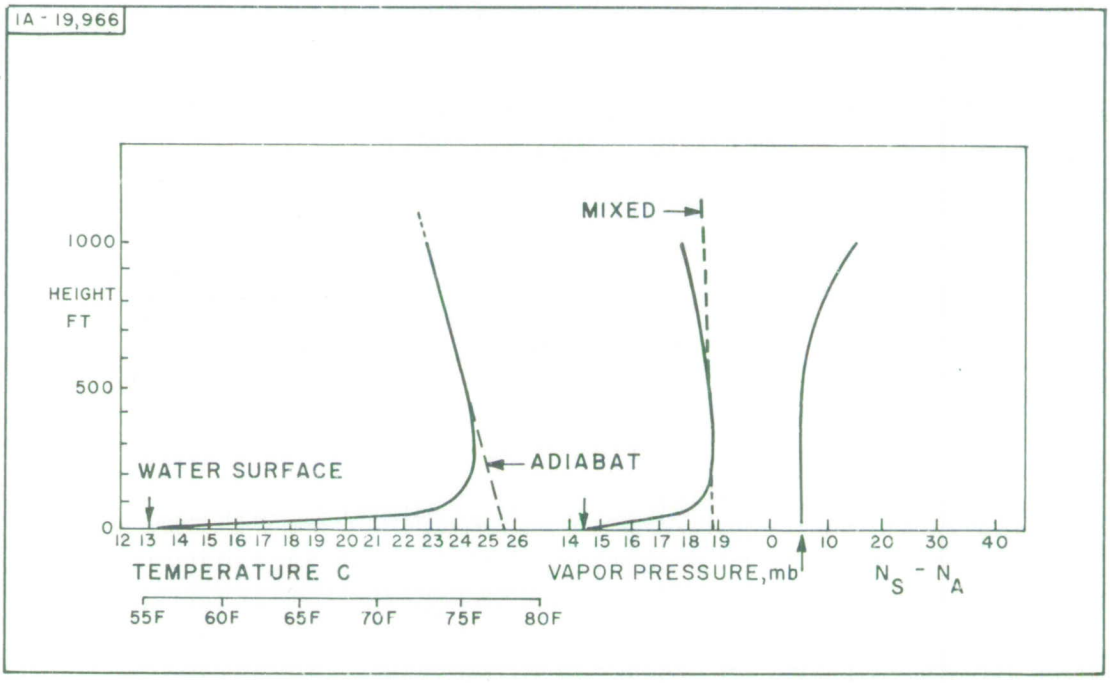

Figure 3. Example of Zero N Deficit

When cool, dry air overflows warmer water the N-deficit would be super-standard and would tend to cause the formation of a surface duct. Due to instability, this duct, if formed, would remain close to the surface, and should eventually dissipate as the air, warmed by the surface, continues to rise.

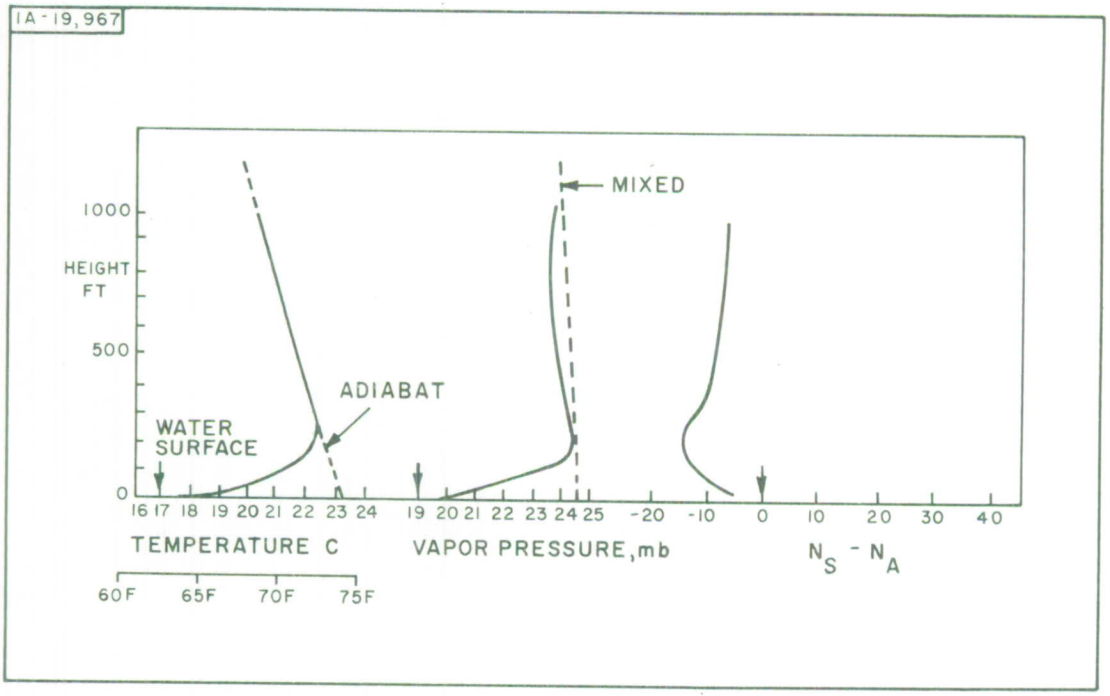

Figure 4. Example of Negative N Deficit

SECTION III

INVESTIGATION OF LAKE SURFACE MEASUREMENTS

In the light of previous discussions it would be useful to categorize the surface measurements and attempt to predict those instances favoring the formation of surface ducts.

Table I shows a list of the temperature excess, N-deficit, wind speed and direction, and wave height for various test periods from 16 September to 8 October 1964. A discussion of the measurements and methods used to derive this data is presented in Appendix II. In all cases, the N-deficit is positive, and the temperature excesses are generally negative, indicating that the overflowing air was, usually, cooler than the water temperature. On the occasion when the air temperature was slightly warmer than the water temperature the wind direction was from the south.

The preponderance of unstable conditions would tend to reduce the probability of strong super-refraction effects extending to any significant level. However, the cases where such situations might occur can be selected on the basis of previous criteria.

(a) a strong, positive N-deficit

(b) near-neutral or stable conditions

(c) low wind speeds

Table I

Cold Lake Surface Measurements

Mission	Date	Time	Wind Speed (M.P.H.)	Wind Direction (Prevailing From)	Wave Height	Temp. Excess (^{o}C) T_a (8 ft) - T_s	N Deficit N_s - N_a (8 ft)
101	Sept. 16	0925	11	SW	Mod.	0.76	14
102	Sept. 17	0957	4	WSW	Slight	0	13
102	Sept. 17	1156	5	WNW	"	0.69	11
102	Sept. 17	1350	4	NW	"	0.87	12
103	Sept. 21	1051	5	S	"	0.69	20
103	Sept. 21	1249	13	S	Mod.	2.13	20
103	Sept. 21	1437	15	S	Mod.	2.24	5
105	Sept. 23	0948	12	W	"	-1.61	22
105	Sept. 23	1145	9	W	"	0.61	23
106	Sept. 24	1217	9	SW	Slight	0.11	21
106	Sept. 24	1354	0	NNE	"	0.34	24
107	Sept. 28	1623	6	N	Mod.	-5.54	27
107	Sept. 28	1803	7	N	"	-5.5	27
108	Sept. 30	1334	5	SE	"	-3.3	18
109	Oct. 1	1619	15	W	"	-2.13	22
109	Oct. 1	1754	*	W	"	-3.52	21
111	Oct. 6	0419	13	S	"	-2.43	20
111	Oct. 6	0602	7	SW	"	-3.04	19
112	Oct. 7	0418	8	NNW	"	-1.82	17
112	Oct. 7	0552	10	NW	"	-2.16	15
113	Oct. 8	0417	5	SE	Slight	-3.78	14
113	Oct. 8	0552	3	ENE	"	-3.99	12
113	Oct. 8	0730	3	E	Mod.	-4.49	13
114	Oct. 8	1610	11	SE	"	4.03	18
114	Oct. 8	1748	9	SE	"	2.03	16
114	Oct. 8	1922	9	E	"	0.90	12

Slight = 6" peak to trough

Mod. = 12" peak to trough

* Wind instrument unserviceable.

On the basis of this selection the following cases satisfy all conditions:

(1) Mission 103 - 21 September - 1051

(2) Mission 106 - 24 September - 1354

The following cases satisfy the same conditions, however the wind speed is somewhat greater:

(1) Mission 103 - 21 September - 1249

(2) Mission 105 - 23 September - 1145

(3) Mission 106 - 24 September - 1217

(4) Mission 114 - 8 October - 1610

In general, based on the surface stability, N deficit and wind speed considerations, Missions 103, 105, 106 and 114 appear to favor conditions for a strong gradient to form over the lake surface. Also because of the large surface N deficits and near-neutral conditions, the gradients could extend to levels well above the surface. [5]

COMPARISON OF LAKE SURFACE MEASUREMENTS WITH INTERFEROMETER RESULTS

The reflection interferometer results, described in Volume I of MTR-118,* illustrated that the larger values of effective earth radii, A_e, represent larger radio-path bending conditions. When experimental interferometer data was obtained with the rays close to the lake surface,

*Available as ESD-TR-67-357, Vol. I (of three volumes).

it was expected that larger values of effective earth radii should correspond with larger values of the surface index gradient.

Table II shows the tendencies for the A_e values to increase, remain constant or decrease as the interferometer signal source approached maximum range (low angle case). From the lake surface (Appendix II) and the radiosonde measurements (Appendix III) the average gradient between the 8 and 539-foot height interval is presented for comparison with the A_e tendencies.

TABLE II

Mission	A_e Tendency At Long Ranges	ΔN Between 8 Ft. and 539 Ft.
102	increasing	average 10
103	varying	11 - 28
104	level	no surface data
105	increasing	10 - 17
106	varying	10 - 19
107	level	8 - 5
108	decreasing	1 - 3
109	level	5 - 10
110	decreasing	no surface data
111	varying	5 - 8
112	level	0 - 8
113	increasing	average 7
114	level	14 - 12

A comparison of data shows that the larger gradients are associated with missions 103, 105, 106 and 114. Referring to the preceding section, it should be noted that lake surface measurements also predicted these missions provided the best conditions for a surface gradient to develop at extended heights over the water. Referring again to Table II, it is apparent that the behavior of the effective earth's radii values is essentially uncorrelated with the magnitudes of the surface gradients. For example, mission 113 indicates that the surface gradient is comparatively low, however, the earth's radius values are increasing with range. Alternatively, for mission 114, with a larger surface gradient there is no increase in A_e values with range.

The apparent lack of correlation between the interferometer measurements of the amount of bending and the surface gradient conditions might be explained as follows. These gradient conditions represent local behavior related to the immediate area of Cold Lake. Ray-tracing results show that for low elevation angles, for example, 3 milliradians, the ray travels a distance of 30 miles before reaching a height of about 600 feet and travels 110 miles to reach a height of 8000 feet. This path geometry is shown in Figure 5. On the average, approximately 1.5 mr total ray bending occurs during the first 30 n. m.

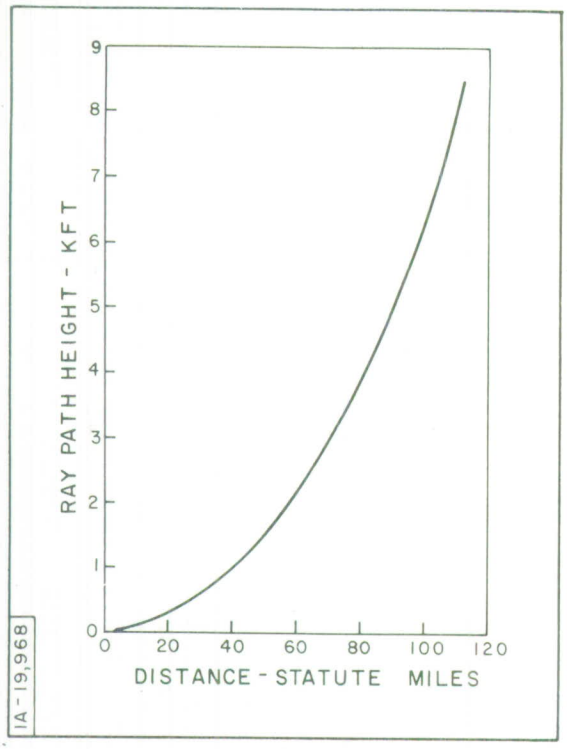

Figure 5. Ray Path Geometry

and about 4.5 mr in the final 80 n.m. Therefore, it is apparent that the overall bending, or in other words, the magnitudes of the effective earth's radii values are very dependent upon the propagation conditions beyond the immediate area of Cold Lake and at heights well above the lake surface.

From Table II a comparison of missions 113 and 114 shows that the surface gradient for mission 114 was larger. However, the interferometer values of the effective earth's radii were not only lower for this mission (see Vol. I, MTR-118), but did not increase with range, as might be expected. Referring to Figure 6, it is apparent

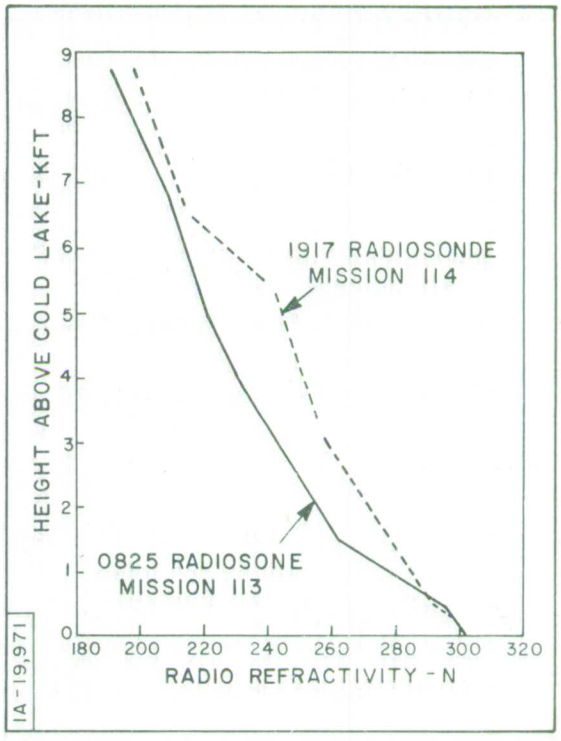

Figure 6. Radiosonde Profiles, Missions 113 and 114

that although the surface gradient is larger for mission 114, the gradient decreases rapidly above 539 feet and in fact decreases again at 3200 feet. The ray-path geometry clearly shows that the bending experienced by the ray above 539 feet is considerably greater for mission 113.

A similar type of comparison can be made between missions 108 and 109. Referring to Table II, the smaller surface gradient exists with mission 108, and the amount of ray bending measured with the interferometer is decreasing with range. With mission 109, however, the degree of bending is essentially constant with range, although the surface gradient is greater.

Referring to Figure 7, it is apparent that the overall refractivity gradient is essentially constant for mission 109, which implies a constant amount of bending with range. The increased bending which occurs because of the surface gradient, apparently does not contribute sufficiently to affect the interferometer data.

However, this is not the case with mission 108. From Figure 8, the variation in the earth's radii data is apparently due to the interaction of a relatively large gradient (-2.06 N/100 ft.) above 500 feet and an extremely low gradient (-0.48 N/100 ft.) below this level. Therefore at 500 feet the magnitude of the gradient increases by 1.58 N/100 feet

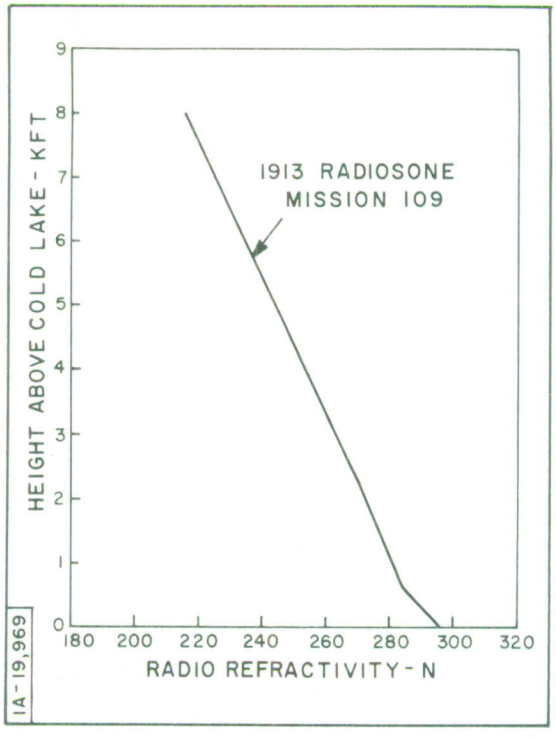

Figure 7. Radiosonde Profile, Mission 109

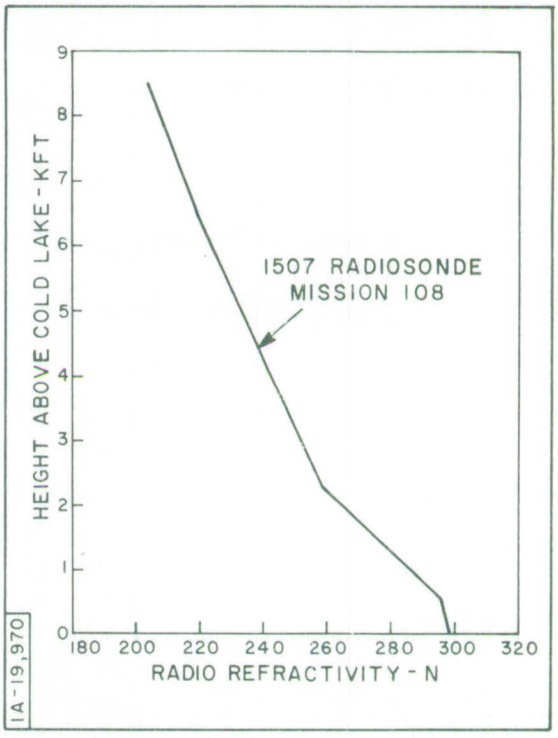

Figure 8. Radiosonde Profile, Mission 108

for mission 108 and is slightly decreased by 0.26 N/100 feet for mission 109.

Referring to Vol I, MTR-118, these A_e values could usually be related to changes in the magnitudes of the gradients at the higher levels. This is an important observation since it implies that it may be possible to determine the effective refractivity profile solely from radio interferometer measurements.

THE ASSOCIATION OF SURFACE GRADIENTS WITH POSSIBLE TRAPPING CONDITIONS FOR THE REFLECTED RAY

Table I shows N-deficit values from 11 to 27 units. The refractivity measurements taken in the air were at a level approxi-

mately 8 feet (2.44 m) above the surface of the water. These values therefore represent surface-level gradients from 4.5 to 11 N-units per meter.

The maximum wavelength which may be trapped by this surface layer and for grazing conditions (Ref. 6, pp 20-21) is given by,

$$\lambda \text{ max} \simeq 0.25 \, (\Delta N)^{1/2} \, d^{3/2} \tag{3}$$

where λ max = wavelength (cms)

ΔN = refractivity gradient (N units/meter)

d = thickness of the layer (meters)

For a layer thickness of 8 feet, i.e., 2.44 meters, and a maximum gradient of 11 N/meter, then

$$\lambda \text{ max} \simeq 3.14 \text{ cms} \tag{4}$$

Since L-band (30 cm) and S-band (10 cm) radio signals were used in the interferometer experiment, it is apparent that the surface-level layer would not have enough thickness to trap the reflected signal.

Referring to the records of the received radio signals (Vol. I, MTR-118) there was no evidence that the reflected ray was ever trapped during S and L band operation. In retrospect it is unfortunate that X band (3 cm) radiation was not available because this wavelength could have approached the condition for trapping.

SECTION IV

CONCLUSIONS

It has been demonstrated that lake surface measurements can be used to determine conditions for large gradients to form over the surface. If the N deficit is large, the stability small, and the wind speed low, the gradient can extend to a considerable height.

Although these predictions were suprisingly good, there was no correlation with the interferometer calculations of the apparent effective gradient. However, it was pointed out from ray-tracing analysis that only a small part of the total bending occurs within the immediate area of the lake surface. At low elevation angles the ray is affected by the propagation conditions extending at least 80 n. m. beyond the lake and by a height interval an order of magnitude greater than the interval (539 feet) over the lake surface.

The earth radii calculations from the interferometer data therefore depend largely upon the conditions beyond the lake surface. However, for short radio wavelengths (3 cms) the surface data is important to define trapping conditions for the reflected ray. Also for long over-water paths and low elevation angles the effects of these surface conditions become very important.

To summarize, the surface conditions during the Cold Lake test did not have a significant impact on the radio path results. This was due to the localized effect of the lake conditions on ray bending and the inability of even strong lake surface gradients to trap S and L band wavelengths.

The largest N change over the 539-foot height interval (28 N units) barely approaches a condition to trap S and L band radiation. However, it is localized to the immediate vicinity of Cold Lake and therefore has insufficient horizontal extent to be very effective.

The results indicate that the interferometer can be used to describe the general behavior of the refractivity gradient at various height intervals (Ref. Vol. I, MTR-118). In addition, fairly simple surface measurements can be used to indicate the strength and extent of the gradient overlying a water surface. This latter determination becomes more effective for extended over-water propagation at low elevation angles.

Together, the interferometer and surface prediction techniques appear to offer a useful method to determine the characteristics of radio propagation conditions with a minimum degree of direct meteorological support.

APPENDIX I

C131 AIRCRAFT INSTRUMENTATION

INTRODUCTION

To determine the absolute value of the index of refraction it is necessary to know the air temperature, air pressure and the water vapor pressure.[7] Relative changes in the index can be measured using a microwave refractometer,[8,9] and the absolute values can subsequently be found by relating the readings at a particular time against an absolute standard. The standard may be at some height on a radiosonde sounding or at low levels by flying the aircraft against instrumentation on a tower. In many applications it is sufficient to know the relative change of index with height, since the index gradient determines the degree of ray bending.[2]

A C131B aircraft was instrumented to make measurements of the above parameters. Figures 9 and 10 show pictures of the aircraft and some of the external probes. In addition, special emphasis was given to the methods for recording data in digital format such that computers could be used to assimilate and process large quantities of data. Analog recordings are used for in-flight observations and to assist in determining the degree of fine structure associated with a given parameter.

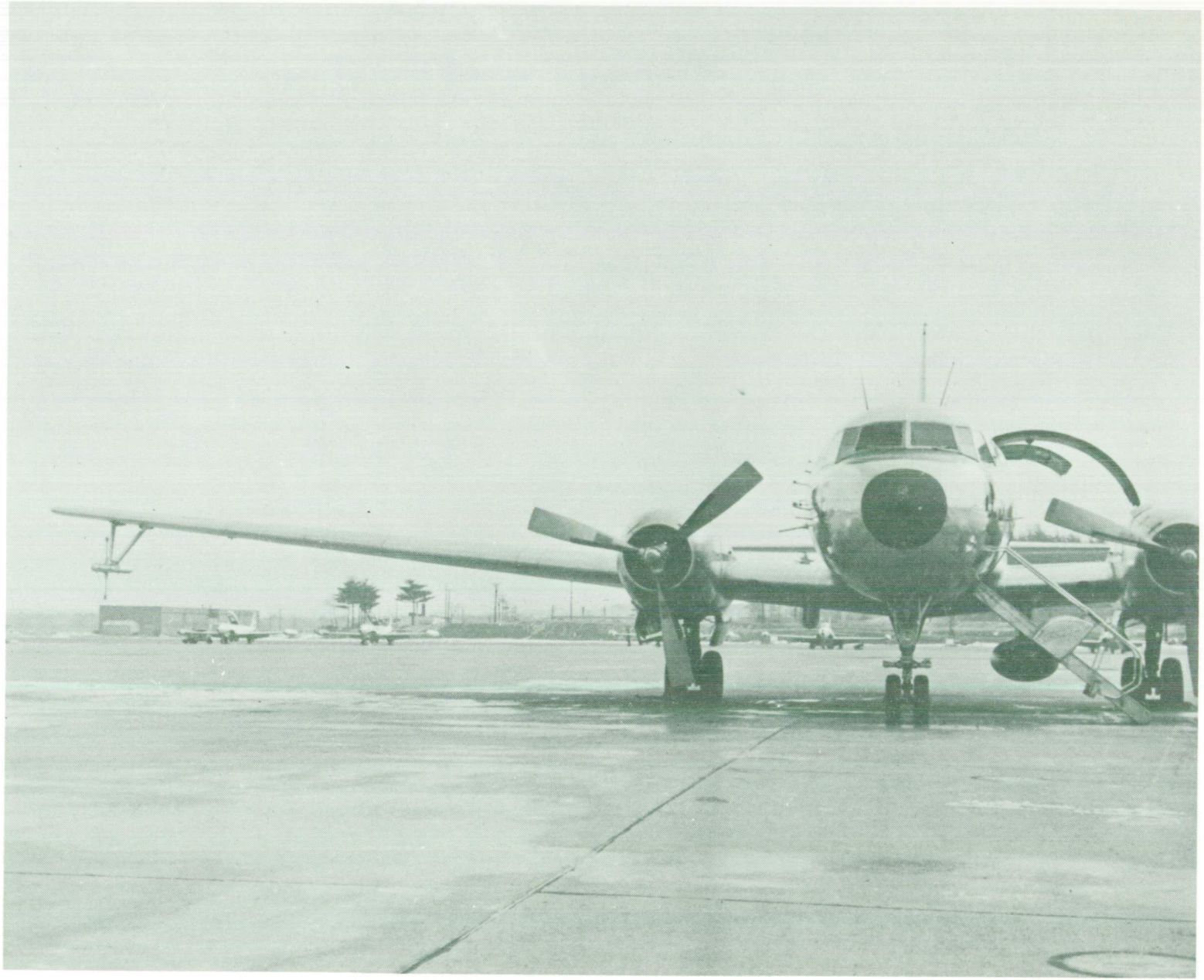

Figure 9. C131 - ESD Aircraft

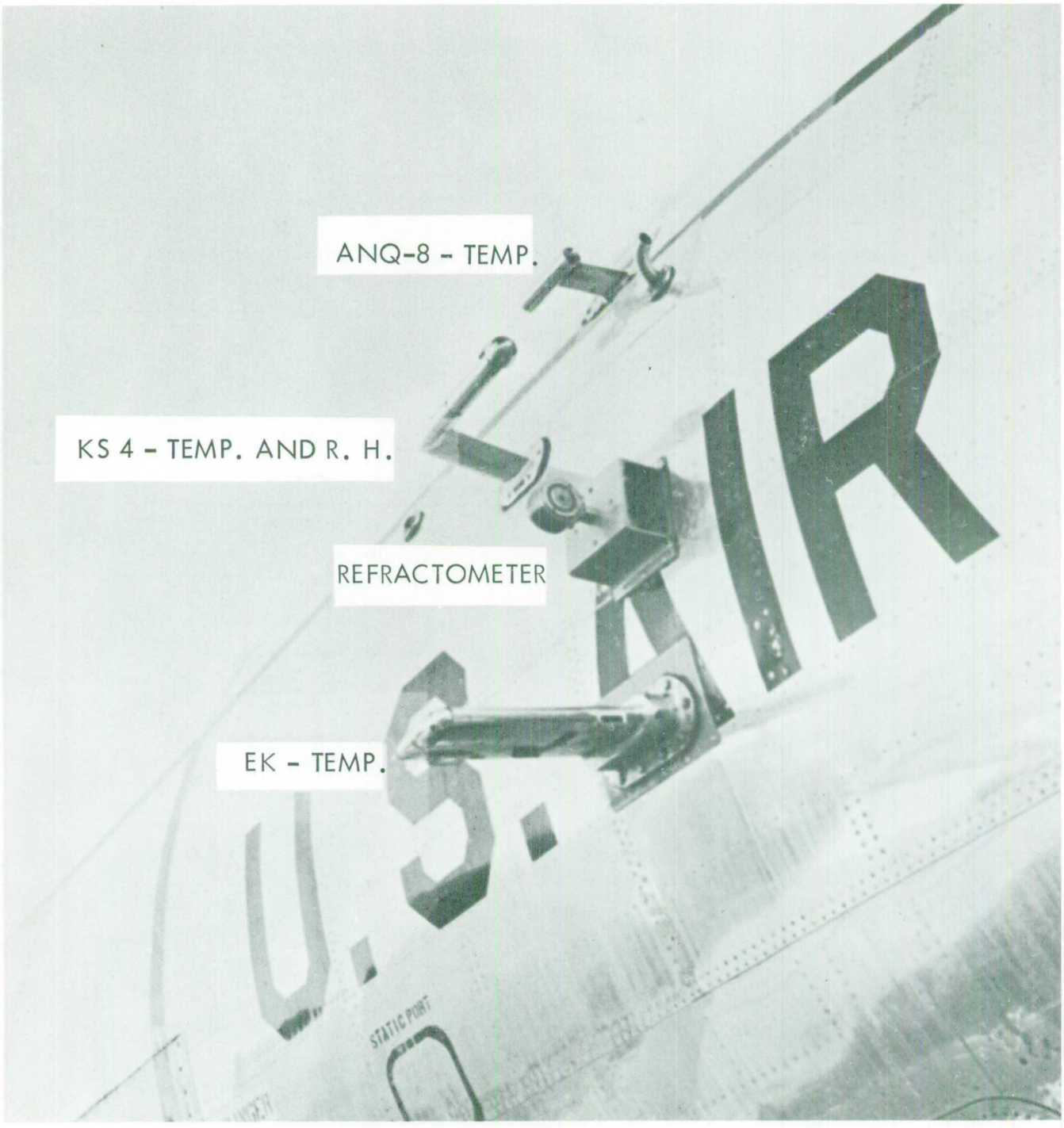

Figure 10. C131 - ESD Aircraft; Probes

The following sections describe the instruments used to measure various parameters and the methods to record and process data.

GENERAL OUTLINE OF INSTRUMENTATION AND MEASURABLE PARAMETERS

Figure 11 shows a general outline of the aircraft installation. The voltage variations from the sensors are recorded on paper chart, magnetic tape, and in digital format on punched paper tape. Table III lists the various parameters which are recorded.

TABLE III

Parameters Recorded by Aircraft Instrumentation

Instrument	Parameter	Frequency Response(Hz)	Accuracy
Digital Clock	Time	---	10^8
Crain Refractometer	Refractivity-N	150*	±0.5N(relative)
SCR-718 Radar Alt.	Height	1	±50 ft.
EK-Platinum Wire	Temperature	8	±0.2°C
AMQ8-Thermistor	Temperature	2	±0.2°C
KS4-Thermistor	Temperature	5	±0.2°C
KS4-Carbon Strip	Relative Humidity	3.25	±10%
Strathan Accelerometer	Vertical Acceleration	2	±0.2g
Giannini Transducer	Airspeed	1	±5 kts.
MKS Transducer	Pressure	1	±0.2 mb.

* Refractometer cavity response less than 10 Hz. [10]

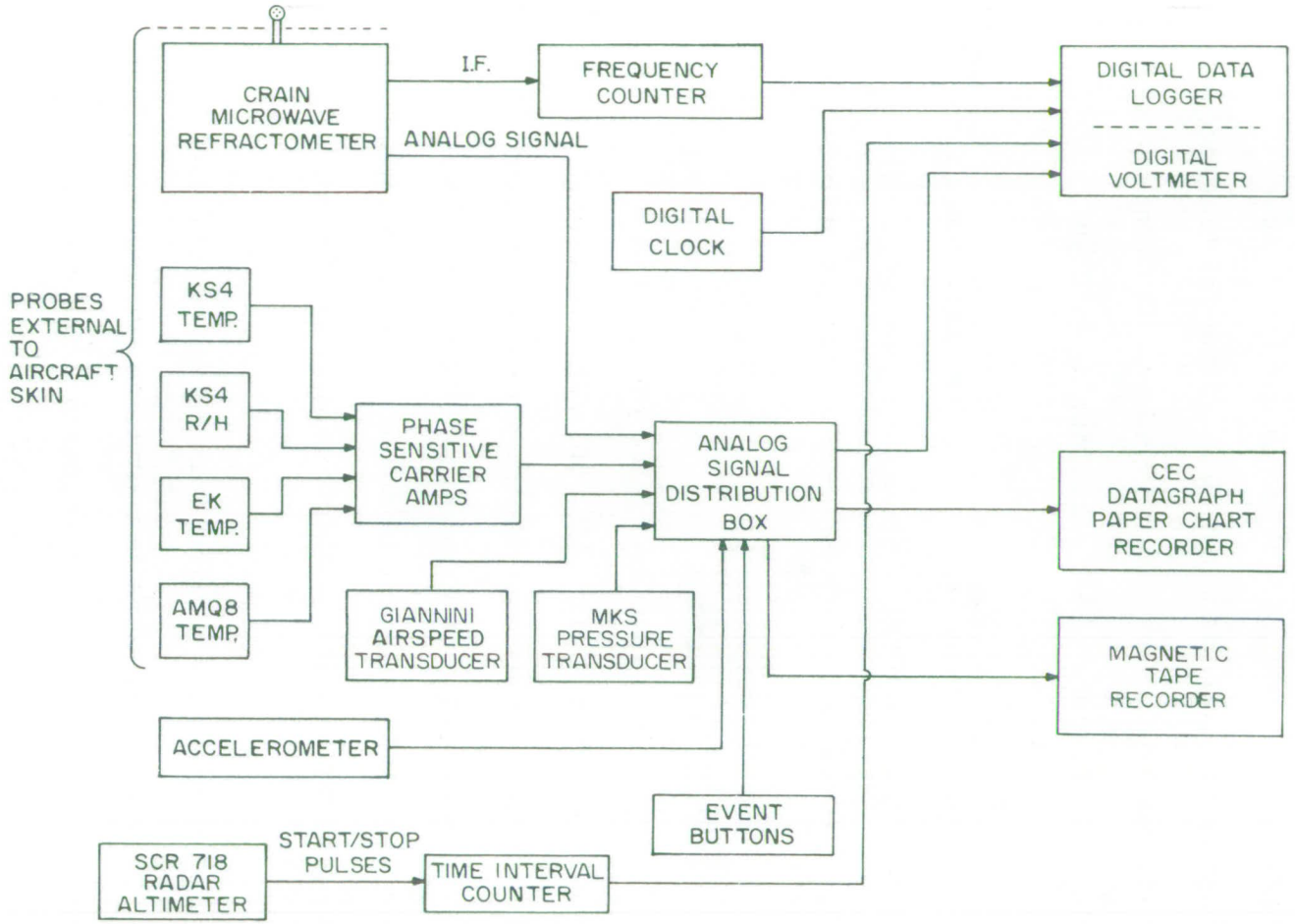

Figure 11. Block Diagram of C131 No 7812 Installation

Paper Chart Recorder

The chart recorder is a CEC model 5-119, optical, oscillograph recorder with 36 channels. The maximum frequency response of the galvanometers is about 30 Hz. One- or ten-second timing marks are recorded on the chart together with event marks to designate special situations which occur during in-flight operation.

The photo-sensitive paper is developed as recordings take place and the information is thereby made available for visual observation during the flight. Figure 12 shows a sample of this recording.

Magnetic Tape Recorder

Analog voltages from all sensors are recorded on a 14-channel Ampex recorder, model AR-800. The frequency response of this instrument far exceeds the signal information bandwidth. A playback system with recorder permits the fine-structure of a selected parameter to be investigated; provision is also made to play the data into a spectrum analyzer for scale-size analysis.

The tape recorder is a valuable back-up to recover data should the other recording systems fail for some reason. Figure 13 shows a sample of index of refraction recordings made from the Crain refractometer and magnetic tape data.

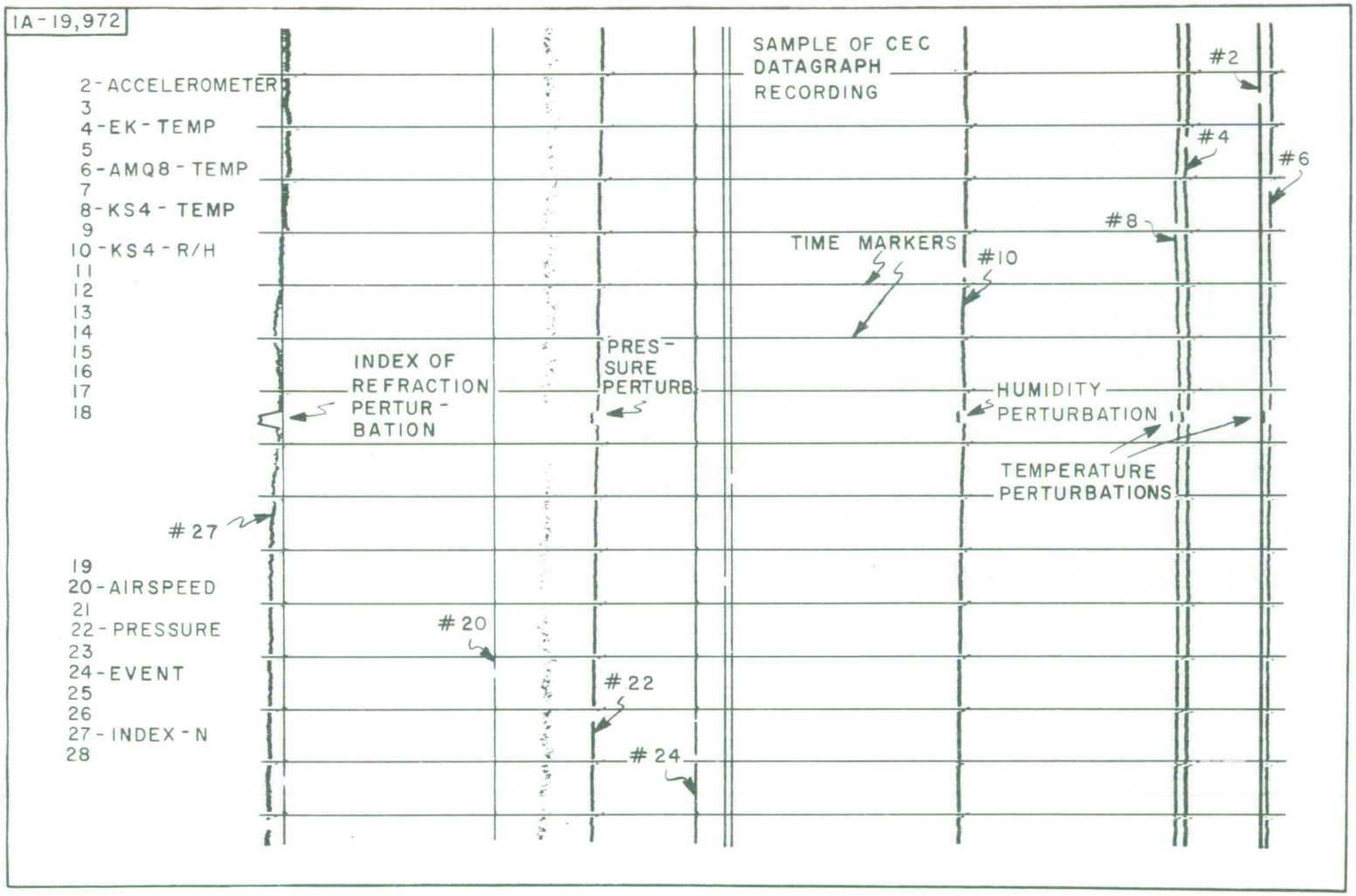

Figure 12. Sample of CEC Datagraph Recording

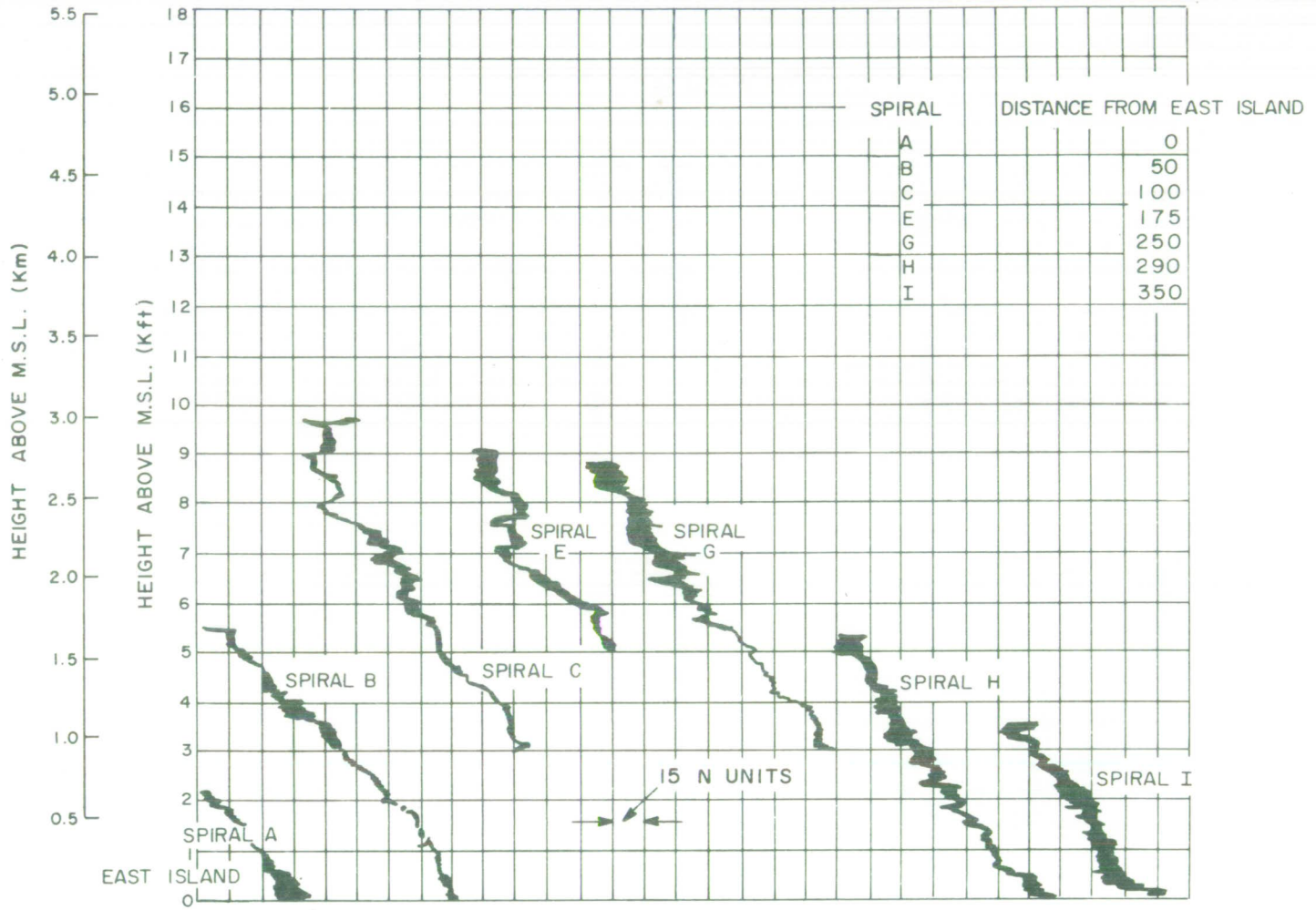

Figure 13. Relative Radio Refractivity Profile

Digital Data Recorder

Analog voltages are converted into digital format using a digital voltmeter. In addition, the IF output from the Crain refractometer is also digitized using a frequency counter. The radar altitude is converted to digital form using a time-interval counter. Therefore both analog signals and raw digital data are fed into the digital data logger. All signal channels are sequentially scanned and the information is punched in paper tape. Figure 14 shows a sample of one complete scan of all channels together with the encoded information.

The recorded data is then transferred onto magnetic tape and can then be processed using a special purpose computer program.

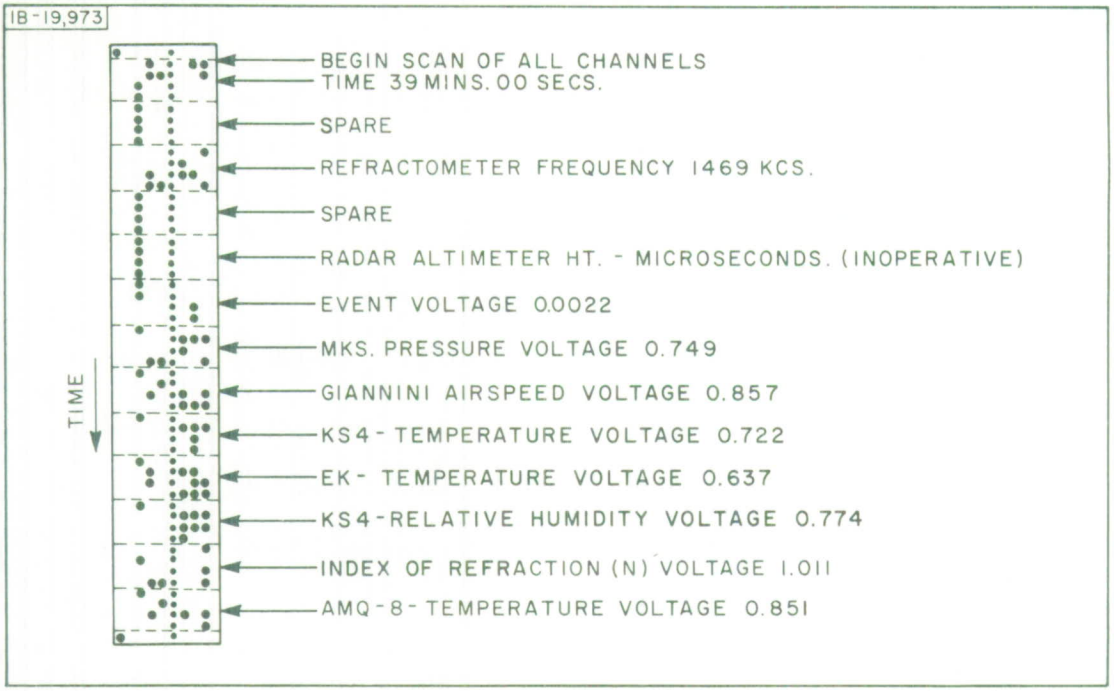

Figure 14. Sample of Digital Tape Recording

ANALYSIS OF DIGITAL DATA

A special-purpose computer program was developed to obtain corrected values of the free-air variables. Each probe is affected by air speed and pressure, and the correction coefficients to remove these errors were determined from calibration flights. For example, in the calibration of the temperature probes, flights were made at various speeds along a path parallel to the isothermal lines obtained from weather maps. The compilation of data eventually yielded a mean value for the correction constant relating temperature variation with air speed. Similar tests were used to determine the correction coefficients applied to the refractometer cavity. Both radiosonde data and low-level flights past an instrumented tower were used to calibrate the various sensors.

The raw data is fed into the computer, corrected, and printed out in tabular form. From the corrected data other meteorological parameters are calculated such as, mixing ratio, potential temperature, geopotential height. Table IV shows samples of the printout which include the raw input data, the corrected data and the meteorological parameters mentioned above. When required, selected parameters may be plotted directly as the data comes from the computer. The most useful data is the average variation of the index of refraction with height. This profile can then be used with a ray-tracing program to determine the amount of radio ray bending and delay when a signal is propagated through the defined medium.

Table IV

Sample of Computer Printout of Processed Aircraft Digital Data

Uncorrected Input Data for the Computation of Free Air Variables

Reading	Indicated Airspeed (knots)	Pressure (mb)	KS4 Temp. (°C)	EK Temp. (°C)	AMQ8 Temp. (°C)	Relative Humidity %	Refractometer Data ΔN	N	Time
1	139.9	806.3	-.5	-3.2	-2.0	100	44.3	251.2	161134
2	140.2	806.3	-.0	-3.0	-1.8	100	45.4	250.1	161136
3	140.0	808.5	.2	-3.2	-2.2	100	47.2	248.3	161138

Corrected Free Air Variables

Reading	Pressure (mb)	KS4 Temp. (°C)	EK Temp. (°C)	AMQ8 Temp. (°C)	Potential Temp - θ (°C)	Calculations Using True Refractometer Data: Mixing Ratio-r (gms/kg)	N Wet	Total N
1	807.3	-2.2	-1.8	-1.6	14.9	2.90	19.0	250.3
2	807.3	-1.7	-1.6	-1.4	15.4	2.80	18.3	249.1
3	809.5	-1.5	-1.8	-1.8	15.4	2.45	16.1	247.3

Corrected Refractive Index Profile and Final Print

Reading	R (Refractivity)	Geopotential Height (Meters)	M (Modified Index)	Potential Temp-θ (°C)	Mixing Ratio-r (gms/kg)	Pressure (mb)	Water Vapor Pressure - e (mb)
1	250.3	1067.0	502.4	14.9	2.90	807.3	3.74
2	249.1	1067.0	501.2	15.4	2.80	807.3	3.61
3	247.3	1045.3	496.0	15.4	2.45	809.5	3.18

Computer programs are also available to permit a correlation analysis of any particular parameter. For example, the auto-correlation function of index of refraction reveals information about the scale-size distribution, limited in its accuracy by the response time of the refractometer cavity.

COMPLEMENTARY EQUIPMENT

A 35-mm camera is located on a gyro-stabilized mount to photograph the earth's surface. This camera has been used to record sea-state and to fix the aircraft position over a particular geographical point. It is particularily useful in the study of land-sea interface investigations where the meteorological measurements may be associated with a precise position at the land-sea boundary.

A drift meter was installed to observe the surface and thereby control the start-stop times of the camera.

Air-inlet and exhaust ducts are available to obtain air samples during flight. This installation, with special filters supplied by the University of Stockholm, has been used to measure gas constituents and isotope content. The air-inlet system will eventually be used with a dew-point hygrometer to make direct readings of the water-vapor pressure.

SUMMARY

Aircraft #7812 has been instrumented to make accurate measurements of atmospheric meteorological parameters, the most important being the index of refraction for ray-tracing analysis. The recording systems are designed to permit visual observations during flight and also to record data for processing in specialized computer programs. For the particular applications in the study of radar errors due to propagation conditions, tropospheric scatter communications and atmospheric measurements the installation has proven itself to be versatile and adequate to meet the assigned missions.

APPENDIX II

COLD LAKE SURFACE MEASUREMENTS

Meteorological measurements were made from an RCAF launch on the surface of Cold Lake during the time radio signal measurements were being made. Psychrometric readings were taken to obtain the refractive index at a height of approximately eight feet above the water surface. Surface water temperature readings were obtained to calculate the index of refraction at the surface. Periodic measurements were made of the wind speed and direction and estimates were made of the lake surface wave conditions.

A list of measured and calculated parameters is shown in Table V.

Table V

Cold Lake Surface Data

Mission	Date 1965	Time L.S.T.	Pressure p(mb)	Dry-Bulb** Temp °C	Wet Bulb** Temp °C	Dew-Point Temp °C	R/H%	Press e(mb)	Refrac. N_a	M.P.H.	Wind Dir.	Wave Cond.*	Surf Water Temp °C
101	9/16	0925	942.1	11.06	9.11	7.39	78	10.291	304.7	11	SW	Mod.	10.3
102	9/17	0957	934.8	11.17	10.00	9.06	87	11.552	308.5	4	WSW	Slight	11.2
102	9/17	1156	935.3	11.94	10.94	10.17	89	12.438	311.4	5	WNW	Slight	11.2
102	9/17	1350	935.1	12.22	11.06	10.17	87	12.438	311.4	44	NW	Slight	11.3
103	9/21	1051	947.1	11.94	9.11	6.61	69	9.7416	302.2	5	S	Slight	11.2
103	9/21	1249	945.1	13.33	10.00	7.17	66	10.151	302.2	13	S	Mod.	11.2
103	9/21	1437	943.1	13.44	12.22	11.33	87	13.383	316.5	15	S	Mod.	11.2
105	9/23	0948	952.5	9.39	6.67	3.89	68	8.0724	299.8	12	W	Mod.	11.0
105	9/23	1145	951.7	11.61	8.11	4.72	62	8.5384	298.1	9	W	Mod.	11.0
106	9/24	1217	945.5	11.11	8.33	5.72	69	9.1542	300.6	9	SW	Slight	11.0
106	9/24	1354	944.4	11.44	8.22	5.17	65	8.8416	298.4	0	NNE	Slight	11.1
107	9/28	1623	952.8	5.06	2.33	1.44	62	5.5138	292.4	6	N	Mod.	10.6
107	9/28	1803	952.7	5.00	2.17	1.67	62	5.3934	291.8	7	N	Mod.	10.5
108	9/30	1334	923.1	6.50	6.11	5.72	94	9.1542	299.2	5	SE	Mod.	9.8
109	10/1	1619	932.1	7.67	5.72	3.67	76	7.9595	294.8	15	W	Mod.	9.8
109	10/1	1754	933.0	6.28	4.72	3.00	79	7.5753	295.5		W	Mod.	9.8
111	10/6	0419	944.9	6.67	4.39	1.67	70	6.9049	294.7	13	S	Mod.	9.1
111	10/6	0602	942.1	6.06	4.28	2.17	76	7.1562	296.1	7	SW	Mod.	9.1
112	10/7	0418	948.7	7.28	5.11	2.67	72	7.4157	298.1	8	NNW	Mod.	9.1
112	10/7	0552	950.0	6.94	5.28	3.44	78	7.7928	300.3	10	NW	Mod.	9.1
113	10/8	0417	951.5	5.22	3.89	2.33	81	7.2074	300.5	5	SE	Slight	9.0
113	10/8	0552	951.3	5.11	4.33	3.44	89	7.7928	303.0	3	ENE	Slight	9.1
113	10/8	0730	951.0	4.61	3.83	2.94	88	7.5218	301.6	3	E	Mod.	9.1
114	10/8	1610	950.0	13.33	8.89	4.67	70	8.5384	298.0	11	SE	Mod.	9.3
114	10/8	1748	950.0	11.33	8.00	4.72	76	8.5384	300.0	9	SE	Mod.	9.3
114	10/8	1922	949.5	10.00	7.78	5.67	83	9.1542	303.0	9.1	E	Mod.	9.1

* Slight - 6 inch peak to trough.
Moderate - 1 foot peak to trough.

** Psychrometric readings taken 8 feet above lake surface.

APPENDIX III

RADIOSONDE DATA

Radiosonde launches were made periodically during the time radio signal measurements were being made at Cold Lake. The launch site was slightly north from Cold Lake and at a height of 539 feet relative to the lake surface.

Additional information such as sky conditions and winds aloft data is available in tabular form at MITRE but has not been included as part of this report.

Radiosonde Data

Mission	Date	Time	Pressure P (mb)	Temperature °K	Temperature °C	Water Vapor Pressure e (mb)	Index of Radio Refractivity N
101	16 Sept.	0908	927	283.8	10.6	7.63	288.4
			900	282.3	9.1	3.79	278.5
			879	282.6	9.4	2.56	253.7
			805	279.2	6.0	0.00	223.8
			760	275.9	2.7	1.77	280.1
			705	269.3	- 3.9	1.99	213.3
			647	265.3	- 7.9	1.34	196.0
			605	264.7	- 8.5	0.90	182.0
			544	262.2	-11.0	0.79	165.0
		1036	927	287.0	13.8	8.36	288.1
			885	282.6	9.4	6.06	271.8
			818	281.5	8.3	2.50	237.6
			754	275.4	2.2	3.85	231.6
			721	273.2	0	3.22	220.9
			652	266.6	- 6.6	2.67	203.7
			588	263.8	- 9.4	1.99	183.6
		1306	926	288.2	15.0	7.58	283.1
			867	283.7	10.5	4.15	256.8
			787	277.4	4.2	3.94	256.8
			764	275.8	2.6	3.20	230.3
			745	274.7	1.5	3.27	226.2
			681	268.4	- 4.8	3.17	213.2
			597	265.1	- 8.1	2.69	189.2

Radiosonde Data

Mission	Date	Time	Pressure P (mb)	Temperature ^{o}K	Temperature ^{o}C	Water Vapor Pressure e (mb)	Index of Radio Refractivity N
102	17 Sept.	0949	920	284.6	11.4	10.57	300.0
			886	280.7	7.5	8.90	286.6
			858	283.6	10.4	9.41	278.8
			804	280.2	7.0	6.38	253.3
			770	278.2	5.0	4.15	234.9
			731	277.8	4.6	4.38	225.1
			690	274.6	1.4	4.72	218.7
			556	262.1	-11.1	1.94	175.1
		1207	920	285.3	12.1	10.87	300.1
			838	281.6	8.4	8.48	271.3
			828	281.1	7.9	7.31	263.1
			725	275.6	2.4	3.53	221.8
			701	274.8	1.6	3.76	216.2
			670	272.4	- .8	4.34	212.8
			562	263.5	- 9.7	2.50	178.6
		1409	920	284.9	11.7	10.94	300.5
			879	280.7	7.5	8.30	281.9
			792	278.7	5.5	5.68	247.4
			756	277.6	4.4	2.42	223.4
			738	277.0	3.8	3.79	225.1
			658	271.1	- 2.1	4.12	209.1
			581	265.1	- 8.1	2.56	183.8

Radiosonde Data

Mission	Date	Time	Pressure P (mb)	Temperature ^{o}K	Temperature ^{o}C	Water Vapor Pressure e (mb)	Index of Radio Refractivity N
103	21 Sept.	1100	932	284.9	11.7	8.19	291.1
			890	278.8	5.6	6.06	276.5
			798	274.3	1.1	4.55	248.4
			772	270.5	- 2.7	3.45	239.2
			737	268.7	- 4.5	2.40	225.4
			672	263.5	- 9.7	0.93	202.6
			660	263.9	- 9.3	0.91	198.9
			600	259.2	-14.0	0.58	182.6
			460	245.0	-28.2	0.19	147.0
		1259	930	286.1	12.9	7.31	285.3
			862	279.4	6.2	5.51	266.0
			782	271.6	- 1.6	4.55	246.7
			722	268.0	- 5.2	2.60	222.9
			700	265.9	- 7.3	2.22	216.1
			622	261.8	-11.4	0.62	187.5
		1518	928	286.6	13.4	8.13	288.5
			866	279.7	6.5	5.47	266.0
			775	271.5	- 1.7	4.31	243.5
			675	263.8	- 9.4	2.54	212.2
			625	261.8	-11.4	1.70	194.3
			566	256.1	-17.1	0.76	175.8

Radiosonde Data

Mission	Date	Time	Pressure P (mb)	Temperature °K	Temperature °C	Water Vapor Pressure e (mb)	Index of Radio Refractivity N
104	22 Sept.	0415	926	279.3	6.1	8.19	296.6
			868	278.6	5.4	7.36	277.6
			661	262.6	-10.6	2.11	207.1
			638	261.8	-11.4	1.99	199.7
			541	252.2	-21.0	0.81	171.4
		0616	927	278.7	5.5	8.60	299.0
			887	276.9	3.7	7.52	284.9
			879	278.0	4.8	8.07	284.2
			812	274.0	.8	4.86	254.0
			631	259.6	-13.6	1.90	199.2
			581	256.3	-16.9	1.34	183.7
		0850	928	280.1	6.9	8.42	297.1
			889	275.6	2.4	6.76	284.0
			829	274.0	.8	5.89	263.9
			664	260.6	-12.6	1.85	208.0
			634	259.1	-14.1	1.35	194.1
			496	246.6	-26.6	0.40	158.7

Radiosonde Data

Mission	Date	Time	Pressure P (mb)	Temperature ^{o}K	Temperature ^{o}C	Water Vapor Pressure e (mb)	Index of Radio Refractivity N
105	23 Sept.	0933	938	281.1	7.9	6.76	290.8
			921	278.2	5.0	5.39	283.0
			868	277.7	4.5	4.83	265.5
			783	270.2	- 3.0	3.07	243.8
			720	266.7	- 6.5	1.61	217.9
			632	259.0	-14.2	0.76	193.8
			564	245.4	-27.4	0.32	180.2
		1145	937	286.0	12.8	6.76	284.7
			872	278.2	5.0	4.51	265.1
			851	276.1	2.9	4.65	261.9
			822	273.8	.6	4.03	252.6
			779	269.8	- 3.4	3.07	240.1
			682	264.2	- 9.0	1.30	207.5
			630	260.2	-13.0	0.65	191.3
		1420	936	286.0	12.8	6.15	281.7
			780	269.8	- 3.4	3.85	244.4
			737	267.2	- 6.0	2.60	227.3
			709	266.4	- 6.8	1.28	213.0
			587	256.4	-16.8	0.48	180.6

Radiosonde Data

Mission	Date	Time	Pressure P (mb)	Temperature °K	Temperature °C	Water Vapor Pressure e (mb)	Index of Radio Refractivity N
106	24 Sept.	1016	931	281.5	8.3	7.31	291.4
			908	278.5	5.3	5.98	282.1
			887	278.2	5.0	5.01	272.6
			775	269.2	- 4.0	3.25	239.9
			752	268.4	- 4.8	2.34	229.5
			674	261.4	-11.8	1.82	210.1
			602	256.7	-16.5	1.38	189.6
			572	254.4	-18.8	1.08	180.7
		1207	931	283.8	10.6	7.26	287.8
			827	273.8	.6	4.86	258.2
			783	271.0	- 2.2	3.56	242.0
			700	264.1	- 9.1	1.85	215.7
			659	260.2	-13.0	1.41	204.2
			638	260.2	-13.0	1.41	197.9
			597	258.6	-14.6	0.91	184.2
		1350	929	286.2	13.0	6.02	279.2
			906	280.4	7.2	5.12	275.3
			837	274.6	1.4	4.31	258.2
			780	270.3	- 2.9	2.56	233.6
			709	264.2	- 9.0	1.98	219.0
			676	261.7	-11.5	1.58	209.4
			605	257.7	-15.5	0.48	184.5
			572	254.9	-18.3	0.36	176.0

Radiosonde Data

Mission	Date	Time	Pressure P (mb)	Temperature ^{o}K	Temperature ^{o}C	Water Vapor Pressure e (mb)	Index of Radio Refractivity N
107	28 Sept.	1613	938	276.5	3.3	4.34	284.8
			802	264.5	- 8.7	2.16	246.5
			764	266.5	- 6.7	0.83	226.7
			741	265.5	- 7.7	0.76	220.4
			650	257.1	-16.1	0.88	201.3
			545	247.6	-25.6	0.21	171.8
		1759	938	273.9	.7	4.03	285.5
			806	264.5	- 8.7	2.34	248.7
			792	263.4	- 9.8	2.33	246.2
			767	266.5	- 6.7	1.40	230.6
			615	265.6	-18.6	0.64	191.2
			590	253.4	-19.8	0.32	182.4
		1934	938	273.4	.2	4.12	287.0
			915	272.6	- .6	3.40	275.0
			802	264.9	- 8.3	2.52	248.4
			784	267.2	- 6.0	2.01	237.8
			760	265.7	- 7.5	1.43	229.5
			696	260.7	-12.5	1.17	213.8
			594	253.1	-20.1	0.31	184.2

Radiosonde Data

Mission	Date	Time	Pressure P (mb)	Temperature ^{o}K	Temperature ^{o}C	Water Vapor Pressure e (mb)	Index of Radio Refractivity N
108	30 Sept.	1324	908	280.5	7.3	9.88	298.4
			865	277.4	4.2	7.58	279.0
			852	278.2	5.0	7.63	274.5
			826	277.4	4.2	4.38	252.5
			805	279.6	6.4	4.09	243.3
			786	279.1	5.9	3.88	237.0
			602	262.3	-10.9	1.17	184.5
			562	259.4	-13.8	0.65	171.7
		1507	907	278.8	5.6	9.09	295.7
			898	277.4	4.2	7.79	289.3
			849	281.9	8.7	5.39	258.8
			783	277.8	4.6	3.73	236.5
			664	266.2	- 7.0	2.13	205.1
			568	258.6	-14.6	0.97	175.8

Radiosonde Data

Mission	Date	Time	Pressure P (mb)	Temperature ^{o}K	Temperature ^{o}C	Water Vapor Pressure e (mb)	Index of Radio Refractivity N
109	1 Oct.	1608	917	279.1	5.9	7.42	290.5
			902	276.5	3.3	5.68	281.2
			812	271.5	- 1.7	4.15	253.3
			726	263.8	- 9.4	2.48	226.7
			659	258.9	-14.3	1.63	206.8
			624	256.7	-16.5	0.84	193.2
			580	251.6	-21.6	0.53	181.8
		1744	918	277.6	4.4	6.43	288.2
			808	268.2	- 5.0	3.79	253.1
			792	268.2	- 5.0	3.73	248.2
			678	260.4	-12.8	1.53	210.4
			612	254.9	-18.3	0.52	189.1
			528	247.0	-26.2	0.28	167.5
		1913	919	276.4	3.2	5.55	285.4
			864	272.9	- .3	4.83	269.5
			799	268.4	- 4.8	3.65	249.8
			712	263.3	- 9.9	2.48	223.4
			600	254.5	-18.7	0.63	186.6

Radiosonde Data

Mission	Date	Time	Pressure P (mb)	Temperature ^{o}K	Temperature ^{o}C	Water Vapor Pressure e (mb)	Index of Radio Refractivity N
110	5 Oct.	0413	945	274.8	1.6	5.16	292.0
			899	275.3	2.1	3.76	272.0
			866	274.5	1.3	2.73	258.6
			810	269.9	- 3.3	3.32	250.3
			748	265.3	- 7.9	1.98	228.9
			685	263.8	- 9.4	0.84	205.9
			666	264.9	- 8.3	0	195.1
			630	263.5	- 9.7	0	185.2
			579	259.2	-14.0	0	173.1
		0628	945	275.6	2.4	5.24	292.3
			934	277.7	4.5	5.35	286.5
			902	276.8	3.6	3.62	270.2
			785	269.3	- 3.9	2.33	238.0
			686	265.9	- 7.3	0.82	204.7
			626	263.4	- 9.8	0	184.7
			517	254.6	-18.6	0	157.7
		0818	945	278.8	5.6	5.72	290.1
			879	275.4	2.2	3.43	264.8
			826	270.4	- 2.8	2.93	252.0
			746	266.1	- 7.1	1.10	223.6
			726	267.0	- 6.2	1.03	216.6
			693	267.3	- 5.9	0	201.0
			625	263.6	- 9.6	0	183.8
			485	253.8	-19.4	0.38	150.6

Radiosonde Data

Mission	Date	Time	Pressure P (mb)	Temperature ^{o}K	Temperature ^{o}C	Water Vapor Pressure e (mb)	Index of Radio Refractivity N
111	6 Oct.	0415	929.9	277.2	4.0	5.98	289.4
			903	284.3	11.1	6.52	276.6
			864	285.4	12.2	6.24	263.6
			784	279.7	6.5	4.25	237.4
			759	280.7	7.5	2.77	222.6
			692	275.0	1.8	3.53	212.6
			632	269.6	- 3.6	3.43	199.6
			621	269.5	- 3.7	1.67	187.5
			533	259.8	-13.4	1.17	165.8
		0611	927	277.3	4.1	6.02	288.8
			888	288.6	15.4	8.72	278.0
			815	283.2	10.0	3.56	239.9
			782	283.3	10.1	2.34	225.2
			716	277.7	4.5	4.25	220.3
			655	273.9	.7	1.80	194.3
			637	272.0	- 1.2	1.34	188.3
			626	270.4	- 2.8	2.33	191.5
			555	263.3	- 9.9	0.78	167.9
		0739	925	278.1	4.9	6.11	287.5
			899	284.7	11.5	9.15	287.6
			874	285.8	12.6	4.34	257.6
			834	286.6	13.4	3.35	241.2
			685	276.7	3.5	1.56	199.4
			636	270.7	- 2.5	2.56	195.6
			585	265.8	- 7.4	1.25	177.4

Radiosonde Data

Mission	Date	Time	Pressure P (mb)	Temperature ^{o}K	Temperature ^{o}C	Water Vapor Pressure e (mb)	Index of Radio Refractivity N
112	7 Oct.	0400	934	281.4	8.2	8.60	298.3
			920	278.6	5.4	6.43	287.6
			861	275.4	2.2	5.64	270.6
			813	274.2	1.0	4.03	250.1
			795	274.3	1.1	3.43	242.0
			750	271.4	- 1.8	3.73	233.4
			697	271.6	- 1.6	1.69	207.9
			638	267.9	- 5.3	0	183.7
			620	268.0	- 5.2	0	179.8
			536	261.5	-11.7	0.87	155.1
		0550	935	276.6	3.4	6.33	293.7
			930	278.7	5.5	6.66	287.7
			826	273.4	.2	4.51	257.1
			812	274.6	1.4	4.51	252.2
			776	273.4	.2	2.84	234.6
			739	271.2	- 2.0	2.54	224.2
			663	270.4	- 2.8	1.09	195.9
			623	267.8	- 5.4	0	180.7
			610	266.5	- 6.7	1.15	183.6
			534	260.9	-12.3	1.30	165.7
		0730	936	277.0	3.8	6.06	291.6
			925	277.2	4.0	6.38	290.0
			846	273.2	0.0	3.73	258.9
			803	274.1	.9	3.94	246.8
			677	271.0	- 2.2	3.22	210.0
			631	268.3	- 4.9	0	183.0
			605	266.0	- 7.2	0.99	181.9
			586	264.1	- 9.1	0.95	177.4

Radiosonde Data

Mission	Date	Time	Pressure P (mb)	Temperature ^{o}K	Temperature ^{o}C	Water Vapor Pressure e (mb)	Index of Radio Refractivity N
113	8 Oct.	0413	937	274.9	1.7	6.11	294.4
			925	281.5	8.3	7.79	292.1
			867	279.8	6.6	4.90	263.5
			837	277.0	3.8	3.67	252.2
			819	278.4	5.2	2.01	238.2
			790	277.7	4.5	0	220.4
			724	274.1	.9	0	204.9
			710	276.2	3.0	0	199.5
			685	275.6	2.4	0	193.2
			608	271.8	- 1.4	0	173.9
			584	269.2	- 4.0	1.19	174.3
		0558	936	274.8	1.6	6.06	293.9
			922	282.5	9.3	8.30	292.4
			840	277.4	4.2	4.90	259.0
			829	279.0	5.8	2.13	240.7
			730	275.2	2.0	0	205.9
			694	276.7	3.5	0	194.3
			629	273.3	.1	0	178.6
			596	270.5	- 2.7	1.40	178.2
		0825	936	277.9	4.7	6.76	293.8
			906	280.6	7.4	0	261.0
			828	278.2	5.0	0	231.0
			795	280.0	6.8	0	220.2
			740	275.2	2.0	0	208.7
			681	278.0	4.8	0	190.0
			632	275.1	1.9	0	178.2
			577	269.8	- 3.4	0	166.2

Radiosonde Data

Mission	Date	Time	Pressure P (mb)	Temperature °K	Temperature °C	Water Vapor Pressure e (mb)	Index of Radio Refractivity N
114	8 Oct.	1559	934	286.6	13.4	6.76	283.9
			899	281.6	8.4	6.43	278.4
			840	279.9	6.7	5.05	256.7
			831	280.4	7.2	4.93	253.6
			786	278.1	4.9	4.31	240.1
			763	279.0	5.8	2.56	224.4
			727	279.8	6.6	3.00	215.7
			661	277.1	3.9	2.25	196.0
			578	268.5	- 4.7	1.38	174.2
		1737	934	283.9	10.7	5.98	282.6
			922	283.7	10.5	6.06	280.8
			866	280.2	7.0	4.79	262.7
			835	281.0	7.8	3.91	248.9
			772	277.7	4.5	3.76	233.6
			720	279.6	6.4	1.63	208.0
			670	277.8	4.6	1.61	194.7
			618	272.7	- .5	1.25	182.4
			484	256.2	-17.0	0.40	149.0
		1917	933	282.2	9.0	7.31	290.8
			915	282.2	9.0	6.61	282.6
			848	281.7	8.5	4.65	255.0
			780	277.2	4.0	4.83	241.8
			745	278.8	5.6	1.72	215.3
			725	279.7	6.5	1.73	209.1
			668	277.6	4.4	1.58	194.0
			575	267.5	- 5.7	0.91	171.5

REFERENCES

1. B. J. Starkey, L. G. Rowlandson, and F/L G. A. Fatum, Cold Lake Radio Propagation and Meteorological Experiment, "Description of a Radio-Meteorological Experiment to Measure Ray-Path Bending in the Troposphere with a Reflection Interferometer," The MITRE Corporation, MTR-118, Volume I, 1 June 1967.

2. M. Born and E. Wolf, Principles of Optics, Pergamon Press, 1959, pp 120-123.

3. E. K. Smith and S. Weintraub, "The Constants in the Equation for Atmospheric Refractive Index at Radio Frequencies," August 1953, Proc. IRE, 41, pp 1035-1037.

4. R. J. List, Smithsonian Meteorological Tables, Publication 4014, the Smithsonian Institution, 1958.

5. R. B. Montgomery and R. H. Burgoyne, Modified Index Distribution Close to the Ocean Surface, Radiation Laboratory of the Massachusetts Institute of Technology, Report 61, February 16, 1945.

6. D. E. Kerr, Propagation of Short Radio Waves, MIT, Radiation Laboratory Series, Volume 13, McGraw-Hill Book Company, Incorporated, 1951.

7. E. K. Smith and S. Weintraub, Proc. IRE, 41, 1960, pp 1035-1037.

8. C. M. Crain, Engineering Report on the Type IV Microwave Refractometer, ECRL Report No. 5-05, University of Texas, 19 Nov. 1954.

9. R. V. Pound, Proc. IRE, 1947, pp 1405-1415.

10. R. O. Gilmer, R. E. McGavin, B. R. Bean, "Response of NBS Microwave Refractometer Cavities to Atmospheric Variations," Radio Science Journal of Research, NBS/USNC-URSI, Vol. 69D, 9, September 1965.

Security Classification

DOCUMENT CONTROL DATA - R & D

(Security classification of title, body of abstract and indexing annotation must be entered when the overall report is classified)

1. ORIGINATING ACTIVITY (Corporate author)
The MITRE Corporation
Bedford, Massachusetts

2a. REPORT SECURITY CLASSIFICATION
Unclassified

2b. GROUP

3. REPORT TITLE
Cold Lake Radio Propagation and Meteorological Experiment (in Three Volumes), Volume II, Determination of Radio Propagation Conditions from Interferometer and Lake Surface Measurements

4. DESCRIPTIVE NOTES (Type of report and inclusive dates)
N/A

5. AUTHOR(S) (First name, middle initial, last name)
Rowlandson, Lyall G.

6. REPORT DATE	7a. TOTAL NO. OF PAGES	7b. NO. OF REFS
August 1967	59	10

8a. CONTRACT OR GRANT NO.	9a. ORIGINATOR'S REPORT NUMBER(S)
AF 19(628)-5165	ESD-TR-67-357, Vol. II
b. PROJECT NO. 7010	
c.	9b. OTHER REPORT NO(S) (Any other numbers that may be assigned this report)
d.	MTR-118, Vol. II

10. DISTRIBUTION STATEMENT
This document has been approved for public release and sale; its distribution is unlimited.

11. SUPPLEMENTARY NOTES	12. SPONSORING MILITARY ACTIVITY
	Deputy for Surveillance and Control Systems, Aerospace Instrumentation Program Office; Electronic Systems Division, L. G. Hanscom Field, Bedford, Mass.

13. ABSTRACT

Reflection interferometer measurements can be used to describe the propagation conditions affecting the degree of ray-path bending. In combination with these measurements relatively simple meteorological measurements at the lake surface can indicate the magnitude of the refractivity gradient and its vertical extent.

In combination, the two methods appear to provide a technique to determine the effective propagation conditions by direct radio signal diagnosis and with a minimum degree of meteorological support.

DD FORM 1 NOV 65 1473

Security Classification

14 KEY WORDS	LINK A		LINK B		LINK C	
	ROLE	WT	ROLE	WT	ROLE	WT
REFRACTION						
PROPAGATION						
Multipath						
Microwave						
Radio						
ATMOSPHERIC PHYSICS						
RADIO-METEROLOGY						